ECS Transactions, 68 (1) 1707-1713 (2015)
10.1149/06801.1707ecst ©The Electrochemical Society

Interdiffusion and Charge Transport Across Surface-Modified Current Collectors in Planar SOFCs

N. Demeneva, D. Matveev, V. Kharton, S. Bredikhin

Institute of Solid State Physics RAS, Chernogolovka, Moscow Distr. 142432, Russia

Current collectors are a key component of planar SOFCs, separating air and fuel supplied onto the electrodes and connecting the cells in series. One of main challenges in the SOFC technology development is to suppress degradation processes, often associated with the interconnect materials, and to provide low contact resistivity in oxidizing atmospheres. The present work is focused on the studies of near-surface interdiffusion phenomena in Crofer 22 APU ferritic steel interconnects with Ni-based protective layers. Particular emphasis was centered on the area-specific resistance (ASR) between the current collectors and $La_{0.8}Sr_{0.2}MnO_3$ (LSM) cathodes, which exhibit time dependencies governed by the protective interlayer composition and interface microstructure alterations. The ASR changes, tested during over 30,000 hours at atmospheric oxygen pressure, can be described in terms of a model assuming that the current across the interconnector | LSM interface is essentially controlled by electron transfer via the interfacial Schottky barrier. The experimental observations validate this approach, explaining the junction resistivity and Schottky barrier height variations as a result of metal interdiffusion between the current collector and Ni-based protective coating.

Introduction

Commercialization of the SOFC technology makes it necessary to reduce costs and to improve performance, reliability and durability of the fuel cell stacks. The most common materials for current collectors of the planar SOFCs operating at intermediate temperatures (750–850°C) are ferritic stainless steels, such as Crofer 22 APU. The choice of such steels is associated, in particular, with their high corrosion resistance at operating temperatures and matching of the thermal expansion coefficients (CTE) with other functional materials. However, the presence of chromium inevitably leads to the formation of Cr_2O_3 oxide scale on the surface, which increases area-specific resistance (ASR) of the interconnector | cathode interface and may cause failure on thermal cycling (1-4). This problem may only be solved employing protective coatings (5). As the interconnect oxidation at the cathode side is responsible for over 30% SOFC stack degradation, the protective coatings minimizing the ASR should provide lifetimes of, at least, 30000 hours (6-10).

In previous works (7,8), a new approach for forming barrier layers impeding Cr diffusion to the metallic current collector surface was proposed and tested. The resultant Ni coatings were found to provide low ASR of the «current collector - LSM cathode»

junctions, varying in the range 5 - 10 mOhm·cm^2 during prolonged tests (up to 30,000 hours) at 850°C in air under a load current of 0.5 A/cm^2. One distinctive feature of these coatings is a significant decrease in their contact resistance at the initial stage (3000 - 5000 h), followed by plateaus-like behavior of the ASR vs. time dependencies when an almost constant resistance is achieved. The present work is centered on the studies of interfacial morphology alterations and charge transport mechanisms associated with these superior properties.

Experimental

Crofer 22 APU (Thyssen Krupp VDM) with 22% chromium content was used as the material for current collectors in the present study. The button samples with a diameter of 18 mm and thickness of 1.5 mm were cut out, polished using a 70 μm diamond grinding disc and then cleaned with an abrasive powder. The discs were dipped into a saturated $NiCl_2$ solution in aqueous HCl, heated up to 70–80°C for surface oxide film removal and adhesion improvement. Then Ni layers (thickness of 6-16 μm) were applied as described elsewhere (7,8). The Ni-coated Crofer 22APU samples were annealed in a vacuum furnace at 1050°C. The microstructural analysis was performed by scanning electron microscopy (SEM) and energy-dispersive spectroscopy (EDS) using a Supra 50VP instrument. The studies of element distribution profiles across the interfaces were carried out after prolonged isothermal treatments at 850°C in air, coupled with electrical measurements as a function of time. In order to detect trace separation of new phases such as Cr_2O_3, micro-Raman scattering spectroscopy was also employed using a Raman fluorescence microscope RamMix M532® (spatial resolution of 1 μm, spectral resolution of 4-6 cm^{-1}).

ASR of the «current collector | $La_{0.8}Sr_{0.2}MnO_3$ (LSM) cathode» couples (Fig.1) was studied as a function of time under the SOFC cathode operation conditions (atmospheric oxygen pressure, 850ºC, current density of 0.5 A/ cm^2). To eliminate the error induced by thermo-emf, the resistance was calculated from the current-voltage dependencies.

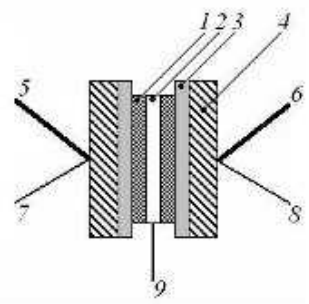

Figure 1. Schematic drawing of the cell used for testing of the protective coatings: (1), porous LSM disk; (2), Pt ring; (3), deposited protective layer; (4), stainless steel disk; (5,6), current leads; (7,8,9), potential probes.

In the course of testing, polished porous $La_{0.8}Sr_{0.2}MnO_3$ disks were symmetrically sandwiched between two coated or uncoated stainless-steel samples. The assembly (Fig. 1) was mechanically loaded with a weight of 2 kg/cm^2 and placed in a quartz chamber

heated up to 850°C. The cell arrangement makes it possible to simultaneously measure resistances of two junctions

(-) Current collector | LSM (+) [1]

with the working polarity corresponding to that under SOFC operation.

Results and Discussion

The ASR vs. time dependences for the junctions of LSM and Crofer 22 APU with the protective layer thicknesses of 16 and 6 μm, are shown in Fig. 2.

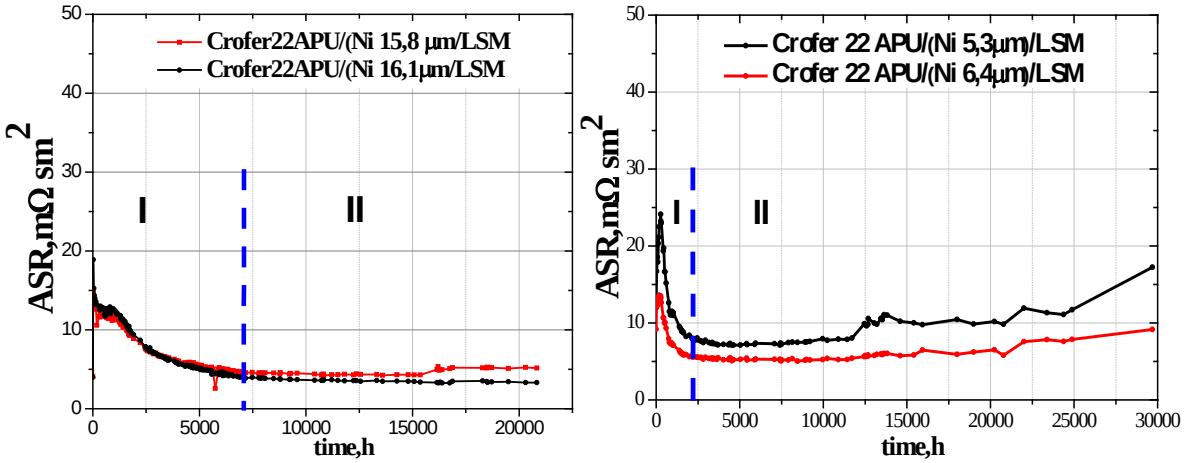

Figure 2. Time dependences of the ASR for the junctions «LSM cathode| current collector» with the protective interlayer thickness of 16 μm (left) and 6 μm (right).

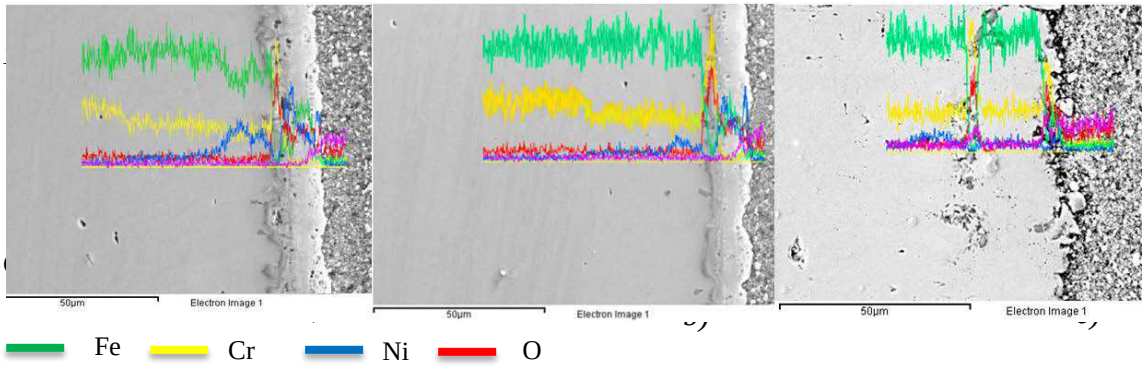

Figure 3. Elemental distribution profiles across the Crofer 22 APU | Ni | LSM junctions after testing during 100 h (a), 400 h (b), and 700 h (c).

As mentioned above, these dependencies can be split into two typical regions with different behavior. During the initial interval (marked as I), the resistivity decreases. The duration of this period of time was shown to increase with increasing thickness of the protective coatings (7,8). One should also mention that the ASR values observed at the end of the first period of time were always similar to one another, 5–7 mOhm×cm^2, irrespective of the starting ASR and Ni layer thickness. After the initial decrease, the resistance tends to stabilize, with a rather insignificant growth during over 15,000-20,000 hours (interval II). The correlation between duration of the initial transient period

and thickness of the protective coatings indicates an important role of interdiffusion. Indeed, the cross-sectional elemental distributions assessed by EDS (Fig.3) clearly show that Ni diffuses into the steel and Fe diffuses in the opposite direction, substituting nickel in the protective layer.

Since the thickness of Ni layer (L) and diffusion time (τ) are known, the diffusion coefficient can be evaluated using the one-dimensional solution of Fick's first law

$$D=L^2/\tau. \quad [2]$$

For 6 μm layer and time interval of 2,500 h, the estimated D is equal to approximately 4×10^{-14} cm^2/s. When L= 16 μm and τ = 7,000 h, the diffusion coefficient of 9×10^{-14} cm^2/s can be found. These values are in agreement with the nickel diffusion coefficients in α-Fe, known in the literature (11).

Figure 4 shows a SEM image with line-scan EDS results for the «Crofer 22 APU with deposited Ni | LSM cathode» junction after testing during 6,000 h. In this case, nickel has already mainly diffused into the stainless steel. One important observation is related to the formation of an additional irregular sublayer between the deposited protective layer and Crofer 22 APU. In fact, this sublayer forms initially when the interdiffusion processes start; then its thickness increases with time (Fig.3).

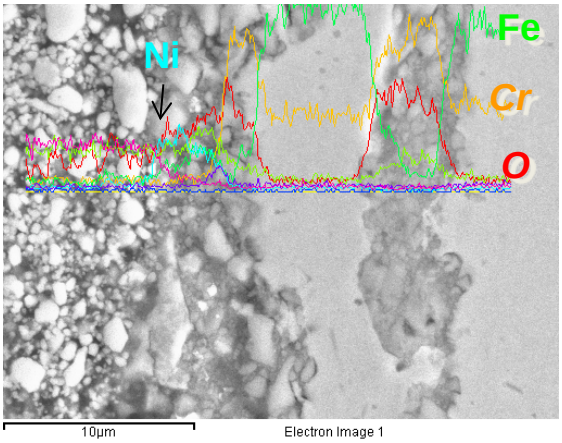

Figure 4. Cross-section and elemental distribution profiles for the junction tested during 6,000 h at 850ºC in air.

EDS analysis demonstrated that the main components of this irregularly shaped sublayer are chromium and oxygen. In order to detect trace separation of new phases, micro-Raman scattering spectroscopy was employed; one example is presented in Fig.5. The local Raman spectrum of the sub-surface island comprises five main lines associated with optical phonons in Cr_2O_3.

The separation of chromium oxide islands at the boundary between the deposited protective layer and Crofer 22 APU agrees well with the mechanism when Ni and Fe interdiffusion plays a dominant role. This mechanism explains also superior stability of the junctions (Fig. 2). At elevated temperatures and atmospheric oxygen pressure, the deposited Ni should be oxidized, forming NiO. However, since chromium has a

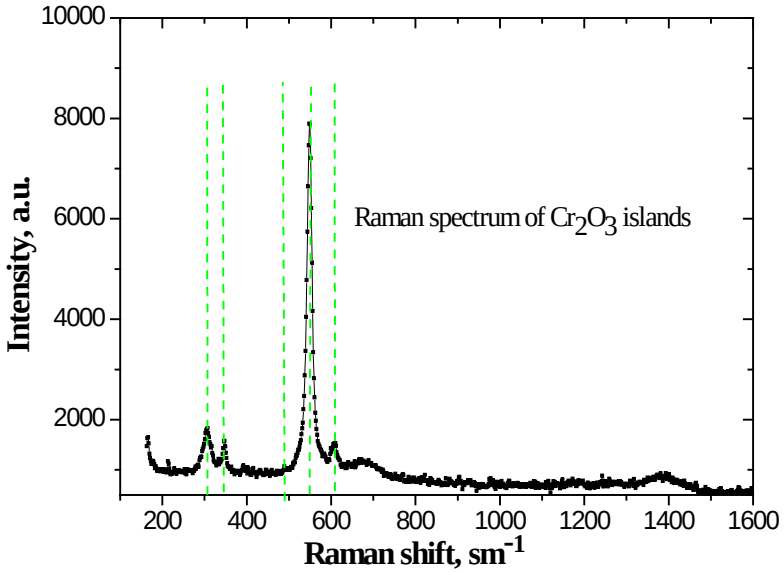

Figure 5. Raman spectrum of a Cr_2O_3 island under the surface of current collector.

substantially lower electronegativity compared to nickel (12), its interaction with NiO should lead to the formation of Cr_2O_3 scale:

$$2Cr + 3NiO \rightarrow Cr_2O_3 + 3\ Ni \qquad [3]$$

Similar reaction is also expected for iron transported in the opposite direction. This interaction enables continuous diffusion of Ni atoms into the bulk of Crofer 22 APU, whilst immobile Cr_2O_3 islands formed at the phase boundary block chromium diffusion to the stainless-steel surface. Although the number and average size of the chromium oxide islands increase with time, the interface remains overall stable.

When discussing the diffusion-affected ASR values, one should note that the total electrical resistance of the «current collector | LSM cathode» assemblies comprises several contributions. These include, at least, ohmic resistance of the stainless steel (R_{Crofer}), ohmic resistance of the porous cathode (R_{LSM}), and a contribution of interfacial Schottky barrier ($R_{Schottky}$):

$$R = R_{Crofer} + R_{LSM} + R_{Schottky} \qquad [4]$$

The former two contributions are time-independent. For the geometry tested in this work, their values can be estimated as $R_{Crofer} \approx 5$ mOhm×cm^2 (13) and $R_{LSM} \approx 0.6$ mOhm×cm^2 (14). The contact resistance can be quantitatively described in framework of the Schottky barrier model for metal– semiconductor interfaces (15-17). The junction between the current collector and SOFC cathode should be considered as forward-biased. In the case of relatively thin blocking layer, the current-voltage relationship and resistance for such a junction can be evaluated as

$$J = AT^2(Ve/kT)exp(-F/kT) \qquad [5]$$

$$R_{Schottky} = \left(\frac{k}{eAT^2}\right) e^{\frac{\Phi_{Metal} - \Phi_{LSM}}{kT}} \qquad [6]$$

where the Richardson constant $A=4\pi emk^2/h^3$ comprises the Planck (h) and Boltzmann (k) constants as well as electron charge (e) and electron effective mass (m); V is the voltage drop across the forward-biased junction; $F = \Phi_{metal} - \chi_{LSM}$ is the difference between the metal work function and electron affinity of the LSM cathodes.

At the interface between LSM and current collector with deposited Ni layer, the ASR value of the Schottky barrier is determined by the work function difference of LSM (Φ_{LSM} ~ 3.9 eV) and Ni (Φ_{Ni} = 5.01 eV) (18). Consequently, for Ni | LSM contact the area-specific resistivity can be estimated as 8.2 mOhm×cm^2; the total ASR of the assembly defined by Eq.[4] is 13.8 mOhm×cm^2. Notice that the experimental values lie in the range 13-18 mOhm×cm^2 (Fig.2).

The same approach can be used to assess ASR after the initial interdiffusion period of time (Interval I in Fig.2), when most Ni is dissolved in the stainless steel and is substituted with iron in the surface layer. For the Interval II, the Schottky barrier becomes determined by the work function of Fe (Φ_{Fe} = 4,81 eV) (18). For the contact between Fe and LSM, the simple estimation gives the Schottky barrier resistivity of 1.05 mOhm×cm^2; the estimated total ASR of the assembly becomes 5.65 mOhm×cm^2. Again, the model provides an excellent agreement with the experimental values, varying in the range 4-6 mOhm×cm^2, Fig. 2.

Conclusions

The area-specific resistance of the "surface-modified Crofer 22 APU current collector | LSM cathode" junctions was studied over long periods of time under the SOFC cathode operation conditions (atmospheric oxygen pressure, 850ºC, current density of 0.5 A/cm^2). The ASR variations can be quantitatively described in framework of the Schottky barrier changes, caused by the work function alterations when Ni diffuses into the stainless steel bulk and is substituted by iron transported from the steel. The microscopic mechanism governing these changes involves also the formation of essentially immobile Cr_2O_3 islands at the boundary between Crofer 22 APU and deposited Ni-based layer. The latter factor prevents chromia transport into porous LSM and, hence, is considered relevant for the stability and electrical resistivity of the interface.

Acknowledgments

This work was supported by the Ministry of Education and Science of the Russian Federation (projects 14.610.21.0007).

References

1. W.Z. Zhu, S.C. Deevi, *Mater. Sci. Eng.*,**348**, p. 227 (2003)
2. K. Fujita., T. Hashimoto, K. Ogasawara, H. Kameda, Y. Matsuzaki, T. Sakurai, *J. Power Sources*, **131,** p. 270 (2007)

3. E. Konysheva, H. Penkalla, E. Wessel, J. Mertens, U. Seeling, L. Singheiser, K. Hilpert, *J. Electrochem. Soc*.**, 153.** p. 765 (2006).
4. S. P. Jiang, J. P. Zhang, X.G. Zheng, *J. Eur. Ceramic Soc.*, **22,** p. 361(2002)
5. J. Wu, X. Liu, *J. Mater. Sci. Technol.*, **26**, p. 293(2010)
6. W.Z. Zhu, S.C. Deevi, *Mater. Res. Bull.*, **38**. p. 957(2003)
7. N. Ledukhovskaya, E. Frolova, G.Strukov, D. Matveev, S. Bredikhin, *ECS Trans.*,.**25.**, 1523 (2009)
8. S.I. Bredikhin, A.A. Zhokhov, E.A. Frolova, N.V. Ledukhovskaya, I.E. Kuritsyna, V.V. Sinitsyn, E.V. Korovkin, *Russ. J. Electrochem.*, **45**. p. 555(2009).
9. V. Sauchuk, S. Megel, E. Girdauskaite, N. Trofimenko, M. Kusnezoff, A. Michaelis , *Russ. J. Electrochem.*, **47**, p. 522.(2011).
10. N.V. Ledukhovskaya, G.V. Strukov, and S.I. Bredikhin, Russian Patent 2011123307 (2012)
11. S. Z. Bokshtein, *Diffusion Processes Structure and Properties of Metals*, Springer (1995)
12. D.R. Lide, *CRC Handbook of Chemistry and Physics*, CRC Press (2008)
13. ThyssenKrupp VDM GmbH, Crofer 22APU data sheet No. 4046, May 2010 edition
14. T. Tsuji; M. Amaya; H. Kamata; Y. Yonemura; J. Mizusaki; H. Tagawa; K. Naraya; T. Sasamoto, *J. Phys. Chem. Solids*, **56**, p. 943 (1995)
15. S. Bredikhin, T. Hattori, M. Ishigame, *Phys. Rev. B*, **50,** p. 2444 (1994)
16. S.I. Bredikhin, V.N. Bondarev, A.V. Boris, P.V. Pikhisa, W. Weppner, *Solid State Ionics*, **81,** p. 19 (1995)
17. F. Salam, S. Bredikhin, P. Birke, W. Weppner, *Solid State Ionics*, **110** , p. 319 (1998)
18. S.Fontana, R. Amendola, S. Chevalier, P. Piccardo, G. Caboche, M. Viviani, R. Molins, M. Sennour, *J. Power Sources*,**171**. p. 652(2007)